LAWRENCE
LIVERMORE
NATIONAL
LABORATORY

UCRL-JRNL-228113

Near-equilibrium polymorphic phase transformations in Praseodymium under dynamic compression

M. Bastea, D. Reisman

February 16, 2007

Applied Physics Letters

Near-equilibrium polymorphic phase transformations in Praseodymium under dynamic compression

Marina Bastea* and D.B. Reisman
Lawrence Livermore National Laboratory, P.O. BOX 808, Livermore, CA 94550

We report the first experimental observation of sequential, multiple polymorphic phase transformations occuring in Praseodymium dynamically compressed using a ramp wave. The experiments also display the signatures of reverse transformations occuring upon pressure release and reveal the presence of small hysteresys loops. The results are in very good agreement with equilibrium hydrodynamic calculations performed using a thermodynamically consistent, multi-phase equation of state for Praseodymium, suggesting a near-equilibrium transformation behavior.

PACS numbers: 64.70.Kb, 62.50.+p, 64.30.+t

The transition metals form an interesting class of materials with complex phase diagrams strongly correlated to the evolution of their electronic structure under applied pressure. Following the enhancement in the *d-band* occupancy, which at lower pressures results in slight atomic re-arrangements in high symmetry structures with negligible density changes, several lanthanides also undergo phase transformations to lower symmetry structures marked by significant volume collapses and a delocalization of the $4f$ electrons [1–3]. Praseodymium (Pr) is a representative example for this type of behavior. Comprehensive theoretical studies up to several Mbars have created a rich basis for understanding both its thermodynamic and electronic properties at elevated pressures [4]. A wealth of static high pressure studies have engaged a range of techniques to map the material behavior under compression. While early experimental studies focused on static pressure conditions [5–9] or nearly-instantaneous shock loading conditions [10], recent developments have enabled explorations on intermediate timescales [11–13].

We carried out comprehensive dynamic compression experiments on high-purity (99.9 %) polycrystalline Praseodymium. Disk shaped samples, 6 mm in diameter and with thicknesses of 0.4 and 0.52 mm, were prepared, metrologized and encapsulated between aluminum (Al) panels and a transparent window, under controlled argon (Ar) atmosphere in order to preclude oxydation. Four identical panels, as shown in Fig. 1, were arranged symetrically around a central cathode to form the anode of the Z-accelerator. The controlled discharge of a large capacitor bank generates a magnetically driven pressure wave with an $\simeq 35GPa$ amplitude and a risetime of $\sim 400ns$, followed by gradual release at the left boundary of the panels, Fig. 1. The loading pressure was carefully designed to avoid field penetration before the end of the experiment, or the development of shocks in the sample, and was monitored on each panel with a reference probe. Variations of $2-3\%$ were registered in the maximum pressure between panels and were ascribed to possible local differences in the corresponding panel/cathode spacing. We measured the velocity of the sample/window interface during the experiment using interferometric techniques (VISAR) [14]. Four interferometer probes were pointed at the center of each sample, with two or more different sensitivities in order to eliminate fringe loss uncertainties. Three types of windows were used in the experiments: [100] single crystal lithium fluoride - LiF, poly-methil-metacrillate - PMMA and z-cut sapphire - Al_2O_3. Their optical properties in the pressure-temperature regime accessed in these experiments have been well studied and are summarized in [15].

As a result of the rapidly applied pressure the samples are compressed along a quasi- isentropic thermodynamic path that intercepts several Pr phase boundaries during both the compressive and subsequent release regimes - see Fig. 2 and the discussion below. As noted in [12] the dynamic impedance of the window plays an important role in the evolution of the phase transformations inside the sample. This effect is clearly illustrated by the present experiments which, as mentioned above, have been carried out with three types of windows: the "stiff" sapphire window produces a significant pressure enhancement at the interface, "soft" PMMA leads to a pressure drop at the interface, while LiF single crystal, relatively closely dynamically matched to Pr, provides a nearly *in-situ* response. The general differences between the experimental traces shown in Figs. 3 and 4 are rather obvious, although they all display the characteristic changes in velocity slope (acceleration) associated with the occurence of phase transitions [12].

The detailed dynamic response of Pr under compression can be better understood by comparing the measured interface velocity $v(t)$ to one-dimensional hydrodynamic simulations mimicking the experimental set-up. We performed such calculations using a multi-phase equation of state for Pr derived from a thermodynamically consistent free energy model [16], Mie-Gruneisen equations of state for the Al panels and windows [17], and the applied pressure history measured by the reference probes. At ambient conditions Pr assumes a *dhcp* structure with initial density $\rho_o = 6.78g/cm^3$, while un-

*Electronic address: bastea1@llnl.gov

der pressure it undergoes a sequence of phase transformations that is specific to the lanthanide series PrI → PrII *fcc* → PrIII distorted-*fcc* → PrIV orthorhombic $\alpha - U$. Several comprehensive studies [1, 6, 8] indicate that the differences between the PrII (*fcc*) and PrIII (*dfcc*) phases are minimal and therefore we used a single representation for them in the model. The PrIII → PrIV transition is marked by a large volume collapse which has been explained in terms of f electron delocalization. Model phase boundaries shown in Fig. 2, are in very good agreement with prior experimental determinations [7, 8]. The principal Hugoniot [10] and the isotherms measured by [8] are also reproduced with better than 2% accuracy.

Our calculations indicate that in the present experiments Pr should undergo two polymorphic phase transformations, at $\sim$ 4GPa and $\sim$ 20GPa, which are marked by slope discontinuities of the interface velocity, e.g. at $\sim$ .12km/s and $\sim$ .56km/s respectively, for the case of a sapphire window, Fig. 4. The experimental $v(t)$ traces clearly exhibit such features, but at slightly larger pressures. An approximately $5 - 10\%$ overcompression, as compared with simulations, is consistently observed in the experiments for all samples and at both (PrI → PrII(III) and PrII(III) → PrIV) phase transformations. We estimate that the PrI → PrII transition occurs in our experiments on timescales $\tau_1 \sim$ 15ns. The τ_1 value was determined as the time between the onset of the discontinuity in the interface acceleration and the subsequent merging of the experimental and simulated $v(t)$ traces, marking the completion of the transformation - see Fig. 4 inset. Similarly, we estimate that *fcc* Pr transforms to the αU phase on a $\tau_2 \sim 10$ ns timescale - see Figs. 3-4, measured again from the $v(t)$ change in slope (i.e. onset of transition) to the discontinuity of the interface velocity signaling the achievement of a fully transformed state. The experimental data show no evidence for significant changes in material properties between 4.5 GPa and 22 GPa, consistent with the initial assessment regarding the similarity of the PrII and PrIII phases. The Al_2O_3 and LiF windows generate the highest pressures in the Pr sample ($\sim$ 55GPa and 40GPa respectively), causing the entire sample to eventually undergo the transformation to the $\alpha - U$ phase. No evidence for additional phase transformations following the formation of PrIV is seen up to 55GPa and $\sim 900K$, the maximum pressures and temperatures achieved in our experiments.

We note that, as indicated by the sample bulk thermodynamic paths in Fig. 2, both the PMMA and LiF windows allow the occurence of the reverse $\alpha - U \rightarrow dfcc$ transformation. In the case of the LiF window, the velocity jump marks the completion of the transition to PrIV in the compressive regime, see Fig. 3. Upon releasing the pressure a short plateau followed by a sudden drop in velocity is observed at $\sim 1.35\mu s$ signaling the onset of the reverse transition at the interface. By comparing the relative positions of the velocity plateau in the experiment and the simulation we estimate that the metastable regime extends below the equilibrium phase line by approximately 1GPa, comparable with the amount of overcompression registered upon crossing the phase boundary in the opposite direction.

The PMMA window is much softer than the Pr and it produces a large pressure drop in the vicinity of the interface. Consequently, the material at and near the monitored surface does not actually transform to PrIV and the signature observed is that of the advancing transformation front in the bulk of the sample [12]. The nearly flat $v(t)$ response between 1.12 and 1.22 μs in Fig. 3 is directly related to the inverse transformation occurring in the bulk of the Pr sample. The reverse transformation most likely completes around 1.28 μs as suggested by the merging of the experimental and equilibrium simulation curves.

Finally, a comparison between the experimental data and hydrodynamic simulations using only a simple, single phase Mie-Gruneisen model for Pr derived from the principal Hugoniot measurements - see Fig. 3, illustrates the sensitivity of the ramp compression technique and its ability to reveal subtle phase transformations. It is worth noting that practically no volume change is detected in static compression experiments for the PrI → PrII transition, the transformation being diagnosed solely on the changes in the diffraction spectrum [9]. Shock Hugoniot measurements have only been able to detect the PrIII → PrIV transition.

In conclusion we report the first observation of sequential, multiple polymorphic phase transformations occuring upon quasi-isentropic compression and release of pure Praseodymium. By employing different windows we probe the effect of boundary conditions on the phase transformation paths and experimental signatures and access three representative regimes. The experimental features on both compression and release are very well reproduced for all windows by a multi-phase, thermodynamically consistent equation of state for Pr. The excellent agreement between experimental data and hydrodynamic simulations suggests that the phase transformations proceed along near-equilibrium paths. We observe small hysterysis loops and estimate the extent of the dynamically explored metastability region around the equilibrium phase boundaries ($5 - 10\%$) of the transition pressure and evaluate characteristic timescales of order $10ns$.

We thank the technical staff at the Sandia Z-accelerator for assistance in executing these experiments. We also thank B. Baer, S. Bastea, P. Springer and D. Young for useful discussions. This work was performed under the auspices of the U. S. Department of Energy by University of California Lawrence Livermore National Laboratory under Contract No. W-7405-Eng-48.

[1] J.C. Duthie and D.G. Pettifor, Phys. Rev. Lett. **38**, 564 (1977).

[2] A.K.McMahan, H.L.Skriver, B.Johansson, Phys. Rev. B **23**, 5016 (1981); H.L.Skriver, Phys. Rev. B **31**, 1909 (1985); A. Delin, L. Fast, B. Johansson, J.M. Wills and O. Eriksson, Phys. Rev. Lett.**79**, 4637 (1997).

[3] N. Tateiwa, A. Nakagawa, K. Fujio, T. Kawae, K. Takeda, Jour. Alloys and Compounds, **408-412**, 244 (2006).

[4] P.Soderlind, Phys. Rev. B **65**, 115105 (2002); A.K.McMahan, C.Huscroft, R.T.Scalettar and E.L.Pollock, Jour. Comput-Aided Mater. Des. **5**,131 (1998).

[5] H.K. Mao, P.M. Bell, J.W. Sittig, J. Appl. Phys. **52**, 4572 (1981); G.S. Smith and J. Akella, J. Appl. Phys. **53**, 9212 (1982).

[6] N. Hamaya, Y. Sakamoto, H. Fujihisa, Y. Fujii, K. Takemura, T. Kikegawa and O. Shimomura, J. Phys. Condens. Matter, **5**, L369 (1993).

[7] Y.C.Zhao, F. Porsch and W.B. Holzapfel Phys. Rev. B **52**, 134 (1995).

[8] B. Baer, H. Cynn, V. Iota and CS Yoo, Phys. Rev. B **67**, 134115 (2003).

[9] N.C. Cunningham, N. Velisavljevic, Y.K.Vohra Phys. Rev. B **71**, 012108 (2005).

[10] W.J. Carter,J.N. Fritz, S.P. Marsh and R.G. McQueen, J. Phys. Chem. Solids, **36**, 741 (1974).

[11] C.A. Hall, J.R. Asay, M.D. Knudson, W.A. Stygar, R.B. Spielman, T.D. Pointon, D.B. Reisman, A. Toor, R.C. Cauble, Rev. Sci. Instr. **72**, 3587 (2001).

[12] M. Bastea, S. Bastea, J.A. Emig, P.T. Springer, D.B. Reisman, Phys. Rev. B **71**, 180101 (2005).

[13] M. Bastea, S. Bastea, J. Reaugh, D. Reisman, submitted to Phys. Rev. Lett.

[14] L.M. Barker, R. Hollenbach, J. Appl. Phys. **43**, 4669 (1972); Hemsing, Rev. Sci. Instr. **50** 73(1979); L.M.Barker *Shock Compression of Condensed Matter - 1997* edited by S.C. Schmidt, D.P.Dandekar and J.W.Forbes (American Institute of Physics, Woodbury, NY, 1998), pp.833-6.

[15] L. Wise, L.C. Chhabildas, in *Shock Waves in Condensed Matter*, edited by Y.M. Gupta (Plenum, New York, 1986), p. 441; D.B. Hayes, C.A. Hall, J.R. Asay and M.D. Knudson, Jour. Appl. Phys. **94**, 2331 (2003).

[16] M. Bastea et al in preparation.

[17] S.P. Marsh, *LASL Shock Hugoniot Data* (University of California Press, Berkeley, 1980).

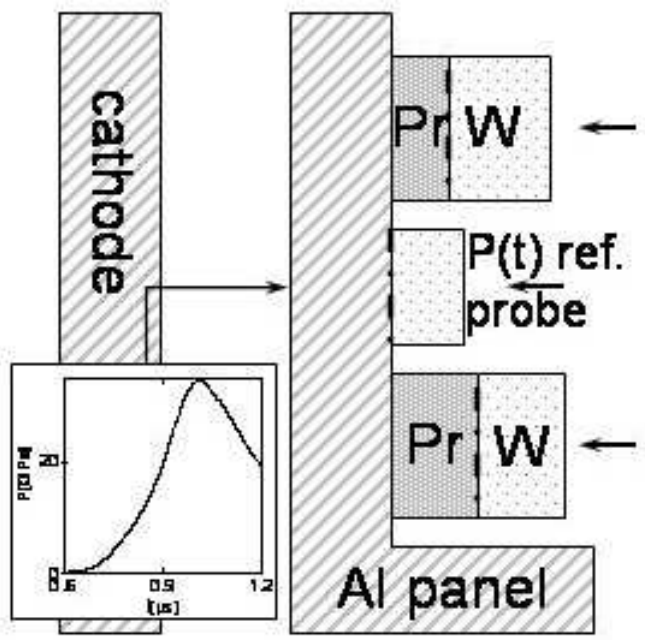

FIG. 1: Schematic cross-section through one of the four the experimental cells (panels) displayed in a square geometry around the cathode of the Z-accelerator. Pr sample (light gray) is encapsulated between the Al panel (1mm thick, dashed) and the transparent window (W: PMMA, LiF or Al_2O_3). A rapidly varying magnetic field in the 3 mm panel/cathode gap generates the compression wave - see P(t) inset. P(t) is measured *in-situ* by the reference probe, a transparent window (LiF) bonded to each panel. Drawing not to scale

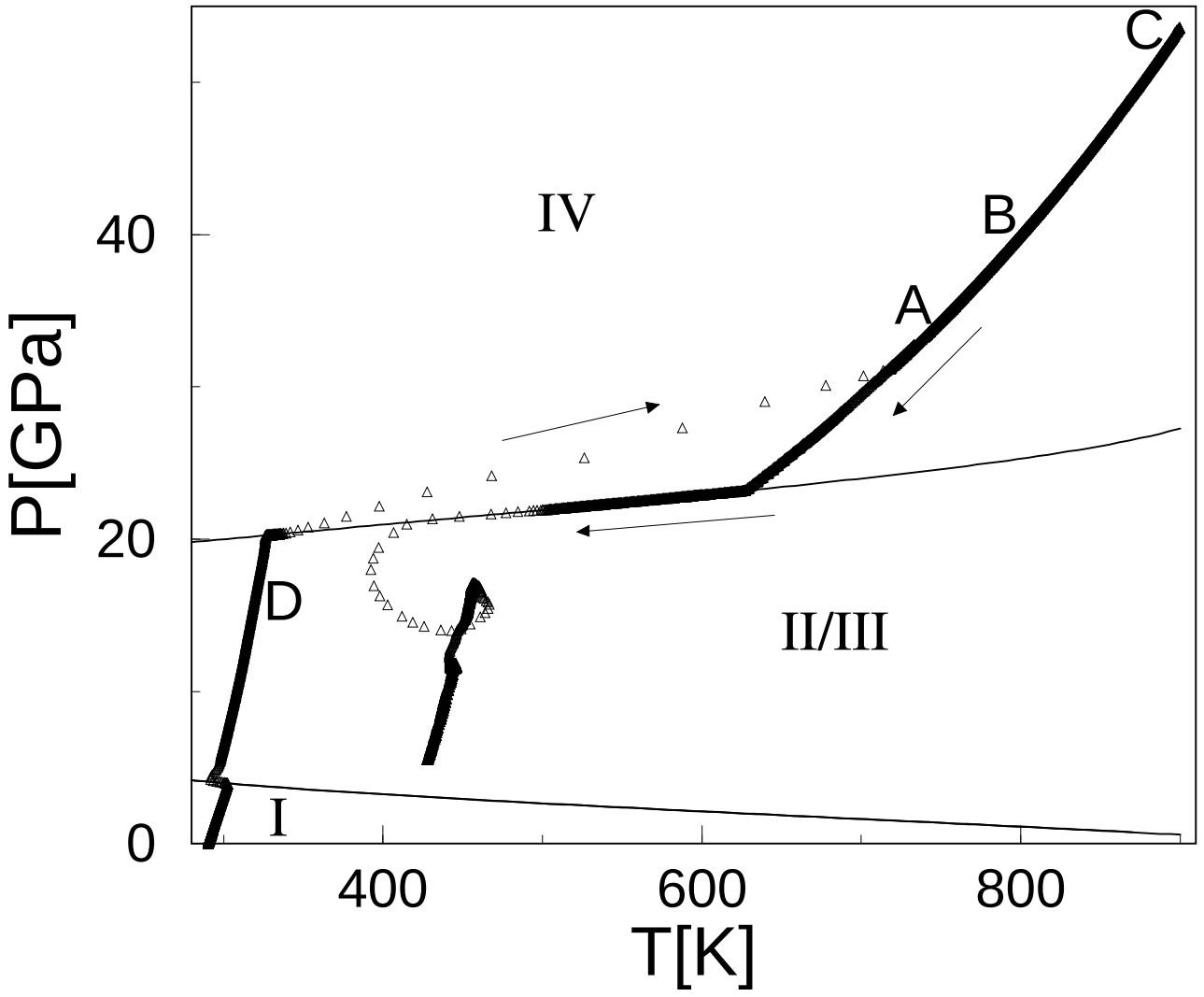

FIG. 2: Model Pr phase diagram and characteristic thermodynamic path (symbols) describing the evolution of the sample. Compression and release paths indicated by arrows. A, B and C mark the maximum pressures achieved with PMMA, LiF and Al_2O_3 windows respectively. D marks the maximum pressure attained at the Pr/PMMA interface - below transformation conditions as discussed in the text.

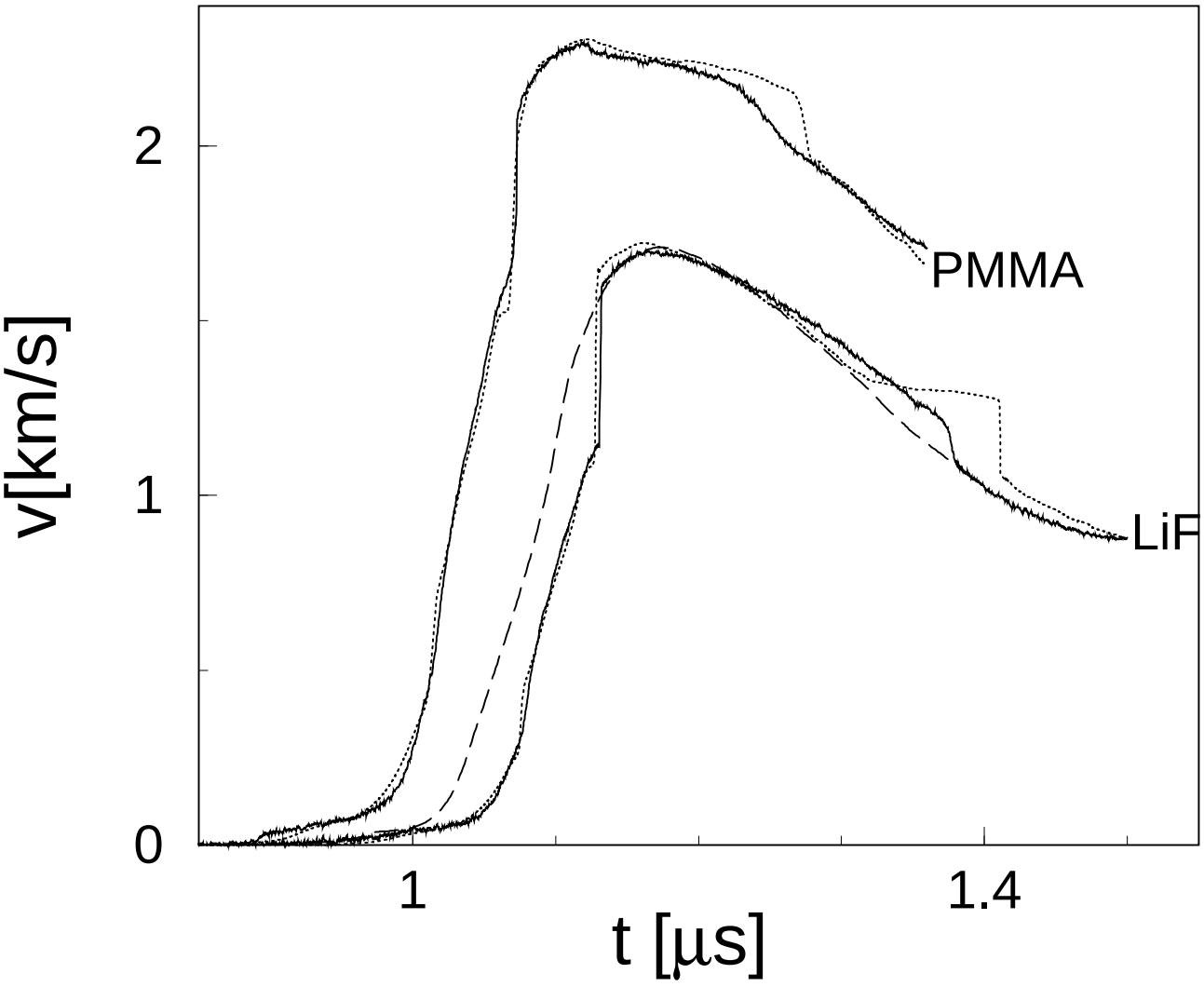

FIG. 3: VISAR traces for the Pr sample with PMMA (t - 50ns) and LiF windows (solid lines) and the corresponding hydrodynamic simulations using the three phase EOS model for Pr (dotted). Dashed curve shows standard hydrodynamic simulation results using a simple, single-phase Mie-Gruneisen EOS for Pr.

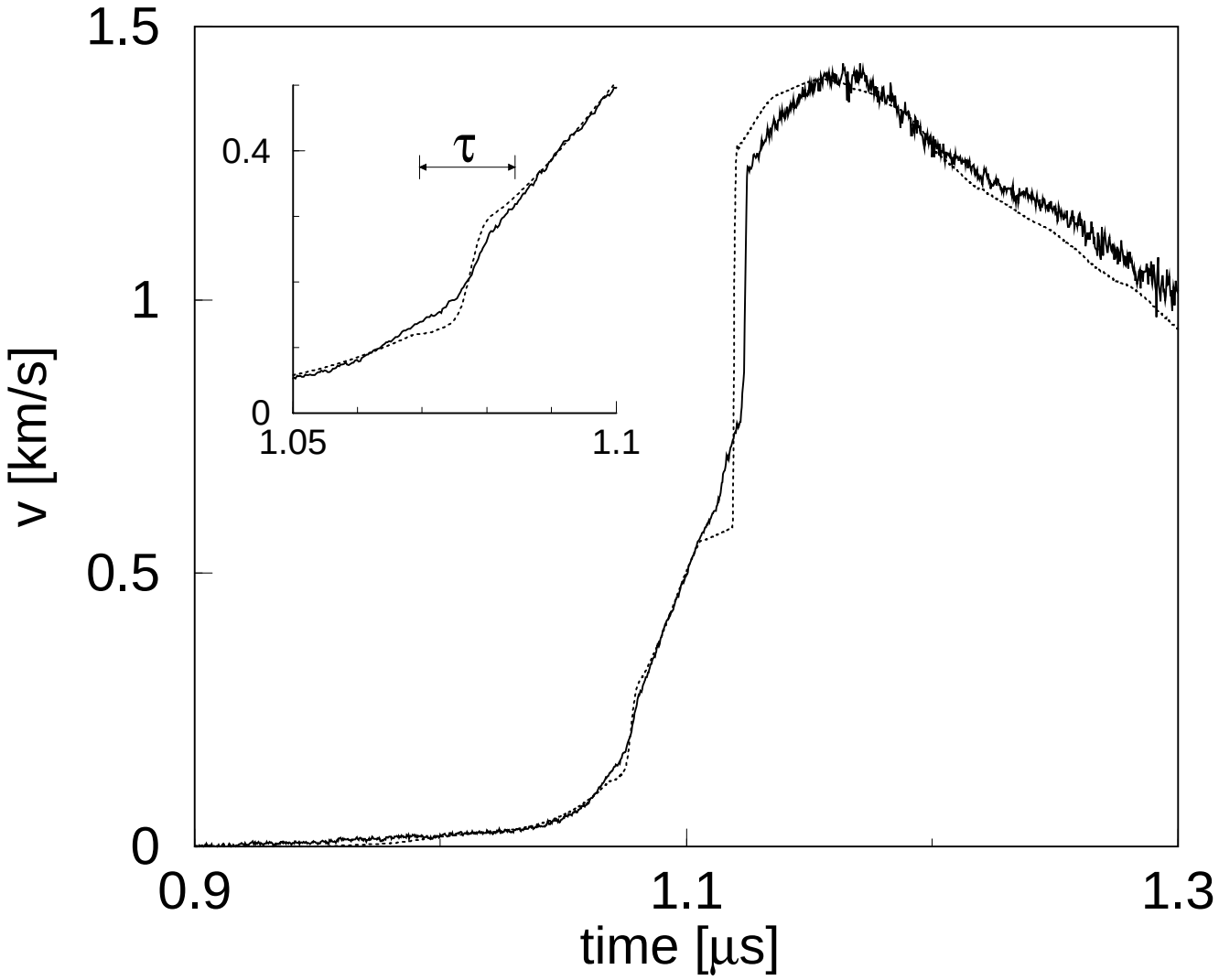

FIG. 4: Measured Pr/sapphire interface velocity - solid lines and simulation results with multi-phase Pr EOS model - dotted lines. Inset details the region of the curve where the first phase transformation occurs.